Check for updates

Response strategies and biological applications of organic fluorescent thermometry: cell- and mitochondrion-level detection

Shuai Li,[a] Yaoxuan Li,[b] Shiji Zhang,[a] Haixiao Fang,[ac] Ze Huang,[a] Duoteng Zhang,[a] Aixiang Ding,[a] Kajsa Uvdal,[d] Zhangjun Hu, [ID]*[d] Kai Huang*[c] and Lin Li [ID]*[ac]

Temperature homeostasis is critical for cells to perform their physiological functions. Among the diverse methods for temperature detection, fluorescent temperature probes stand out as a proven and effective tool, especially for monitoring temperature in cells and suborganelles, with a specific emphasis on mitochondria. The utilization of these probes provides a new opportunity to enhance our understanding of the mechanisms and interconnections underlying various physiological activities related to temperature homeostasis. However, the complexity and variability of cells and suborganelles necessitate fluorescent temperature probes with high resolution and sensitivity. To meet the demanding requirements for intracellular/subcellular temperature detection, several strategies have been developed, offering a range of options to address this challenge. This review examines four fundamental temperature-response strategies employed by small molecule and polymer probes, including intramolecular rotation, polarity sensitivity, Förster resonance energy transfer, and structural changes. The primary emphasis was placed on elucidating molecular design and biological applications specific to each type of probe. Furthermore, this review provides an insightful discussion on factors that may affect fluorescent thermometry, providing valuable perspectives for future development in the field. Finally, the review concludes by presenting cutting-edge response strategies and research insights for mitigating biases in temperature sensing.

[a]The Institute of Flexible Electronics (IFE, Future Technologies), Xiamen University, Xiamen 361005, China. E-mail: ifelli@xmu.edu.cn

[b]Department of Health Statistics, School of Public Health, Shanxi Medical University, Taiyuan, China

[c]Future Display Institute in Xiamen, Xiamen 361005, China. E-mail: k_huang@xmu.edu.cn

[d]Department of Physics, Chemistry and Biology, Linköping University, Linköping, 58183, Sweden. E-mail: zhangjun.hu@liu.se

Shuai Li received his bachelor's degree in materials physics from Shaanxi University of Science and Technology (China) in 2023 and then pursued his master degree at Xiamen University (China). His main research interests lie in the synthesis and biological application of fluorescent temperature probes.

Shuai Li

Zhangjun Hu received his B.S. degree (2002) and PhD (2008) from Anhui University, and Docent from Linköping University (2018). He had been Postdoc Fellow at Tongji University (2008–2010) and Linköping University (2010–2014), and Assistant Professor at Linköping University (2014–2018). Since 2018, he has held the position of Associate Professor at the Molecular Surface Physics and Nanoscience (MOLYT) division, IFM, Linköping University. His current research interests focus on molecules, complexes, and nanomaterials for biomedical imaging/ sensing and functional materials for new sustainable purposes.

Zhangjun Hu

1 Introduction

Temperature is a crucial parameter reflecting the state of biological and physiological functioning, closely associated with heat.[1,2] Cells, the fundamental units responsible for bodily functions,[3] derive their temperature primarily from energy metabolic processes.[4] Mitochondria, recognized for releasing a significant amount of heat through the process of oxidative phosphorylation and various biochemical reactions, play a pivotal role in maintaining temperature homeostasis within the entire cell.[5,6] In normally functioning cells, variations in the number and activity of mitochondria contribute to temperature differences across cells and organs.[7] The obstruction of heat transfer by cytoplasmic and biological membranes results in a mitochondrial temperature different from cellular temperature.[8,9] In contrast, in diseased cells associated with mitochondrial dysfunction, the disruption of their energetic state[10] results in a disturbance in temperature homeostasis. For instance, individuals diagnosed with mitochondrial diseases often exhibit a notable decrease in brain temperature due to impaired oxidative phosphorylation.[11,12] Cancer cells and inflammatory cells, in contrast, exhibit enhanced mitochondrial metabolism, resulting in elevated cellular temperatures.[13,14] Therefore, mitochondrial temperature emerges as a crucial indicator for evaluating the functional status and metabolic level of biological tissues.[9] The accurate real-time detection of mitochondrial temperature can not only aid the comprehension of functional variability in various biological tissues with temperature but can also facilitate the exploration of the association between mitochondrial dysfunction and temperature abnormalities. This, in turn, can offer *in vivo* diagnosis strategies for related diseases.

Compared to conventional temperature detection methods, such as thermocouples and infrared sensing,[15] fluorescent thermometry has become an essential tool for cellular and mitochondrial temperature detection. This is attributed to the inherent advantages of fluorescence technology, including its low biological invasiveness, high resolution, and high sensitivity. Various materials have been employed to develop different fluorescent thermometers, including organic dyes,[16] vacancy-containing nanodiamonds (NDs),[17] quantum dots (QDs),[18] upconversion nanoparticles (UCNPs),[19] and lanthanide-doped materials.[20] Despite the high accuracy of lanthanide-doped materials in temperature detection, their fluorescence quantum yield and controllable targeting properties are not ideal. However, inorganic materials, including NDs, UCNPs, and QDs, present challenges related to non-invasive cell delivery,[21] low localized heating,[19] and low photobleaching,[18] respectively. Compared to these materials, small-molecule probes stand out for their short response times, good biocompatibility, and flexible structures. On the other hand, the thermoresponsive properties of polymers enable additional temperature-dependent variables to be determined, such as polarity and viscosity. Moreover, polymers can be integrated with other probes for detecting biological targets, creating a multifunctional sensing system. Their design flexibility and outstanding photophysical properties make both small-molecule and polymer probes promising alternatives for intracellular temperature detection. In the presence of light of the appropriate wavelength, electrons in the highest molecular orbital (HOMO) will jump to the lowest vacant orbital (LUMO). During the return of the electrons from the excited state to the ground state, the excess energy is released in the form of fluorescence. Therefore the fluorescence process of the probes involves the excitation of electrons to a higher energy state upon the absorption of a photon, followed by the release of the photon upon return of the electron to a lower energy state.[22] In addition, the selection of proper fluorescent parameters is a crucial consideration. Currently, fluorescence intensity and lifetime methods have been developed for temperature detection. Fluorescence intensity detection is characterized by its simplicity of operation; however, its accuracy can be susceptible to microenvironment influences.[19] In contrast, fluorescence lifetime methods, being independent of the concentration, enable increased accuracy in temperature detection.[23]

Existing reviews have primarily documented the development of fluorescent temperature probes based on factors such as the number of emission wavelengths[24] and the selection of

Kai Huang earned his PhD in physics from Nanjing University in 2007. Then he obtained his academic position in Xiamen University and was promoted to a professor in 2016. His research interests focus on wide-band-gap semiconductor light-emitting diodes, photodetectors, and fundamental physics in surface plasmon behaviors.

Kai Huang

Lin Li received his BSc degree and PhD in chemistry from Anhui University in 2004 and 2009, respectively. He then carried out postdoctoral studies with Prof. Shao Q. Yao at NUS. He got his professor position at Nanjing Tech University in 2015 and adjunct professor position at Northwestern Polytechnical University (NPU) in 2018. Then, he moved to Xiamen University in 2023 as a professor. His research group focuses on mito-

Lin Li

chondrial information and health engineering.

small-molecule dyes.[25] Despite these contributions, the understanding of the principal differences between temperature-response strategies remains unclear. The thermosensitivity exhibited by fluorescent temperature probes is ascribed to different response strategies in photophysical processes.[26] Consequently, the present review summarizes in detail the underlying principles of the reported response strategies. Additionally, it briefly outlines the biological applications of various types of probes. Ultimately, the review considers the future development prospects of rationally designed fluorescent temperature probes to effectively address the challenge of accurately detecting mitochondrial temperature.

2 Fluorescent thermometry at the cell scale

Energy metabolism during cellular physiological activities, such as ion cycling, signaling, and cellular respiration, leads to the generation and release of heat, which in turn induce fluctuations in temperature.[27] The accurate analysis of intracellular temperature can provide a new understanding of temperature-dependent cellular activities. The non-invasive fluorescent temperature probe is one of the practical/feasible tools for intracellular temperature measurement. Overall, it facilitates the real-time temperature monitoring of cellular processes based on the mechanism of intramolecular rotation, polarity sensitivity, and Förster Resonance Energy Transfer (FRET).

2.1 Intramolecular-rotation-based temperature probes

External conditions, such as viscosity, temperature, and ionic strength, have the potential to induce the rotation and vibration of fluorescent dyes, leading to fluorescence quenching through nonradiative relaxation processes.[28–30] However, this phenomenon can be applied as a response mechanism for designing probes. Fluorescent temperature probes based on intramolecular rotational design rely on the rotational rate of the sensitive units to generate fluctuations in fluorescent parameters. Thus, the selection of the probe favors fluorescent dyes with molecular rotors or notable aggregation-induced emission (AIE) properties.

As shown in Fig. 1, most intracellular fluorescent temperature probes are based on rhodamine, BODIPY, or AIE dyes. The temperature response is typically accomplished through intramolecular rotation or restricted intramolecular rotation (RIR). However, challenge arise from complex microenvironmental factors, such as pH and viscosity, which may introduce bias during the temperature measurement. Therefore, additional rational chemical modifications of the fluorescent probes are often required to ensure the specificity of the temperature response.

For rhodamine dyes, the rotation of the diethylamino moiety is temperature dependent. As the temperature rises, nonradiative relaxation from intramolecular rotation increases, leading to a decrease in the fluorescence intensity and lifetime. Dmitriev et al. reported a sulforodamine-based fluorescent temperature probe (1), using a single-wavelength fluorescence

lifetime and intensity as the temperature-sensitive parameters.[31] The design of the sulforodamine, incorporating a hydrophobic aliphatic tail, facilitated the entry of the dyes into polymer nanoparticles through co-precipitation. This design addressed a challenge faced by conventional rhodamine derivatives, which typically exhibit good water solubility, making their incorporation into polymers more challenging. Additionally, the lipophilicity of probe 1 could effectively prevent leakage from the nanoparticles. Embedding the dyes in polymer or silica nanoparticles is an effective method to avoid potential intracellular interference. However, nanoparticles aggregation in the cytoplasm can affect signal detection, and the larger size of particles tend to exhibit heterogeneous dispersion. Therefore, when designing fluorescent temperature nanoprobes using the encapsulation of fluorescent dyes, the cell membrane permeability and dispersion in the cytoplasm must be taken into account. Differently, Takai et al. reported a fluorescent temperature probe (2) consisting of an amphiphilic block copolymer loaded with a thermosensitive dye (rhodamine B) and an internal reference dye (coumarin).[32] The self-assembly under aqueous conditions forms nanoparticles, providing a protective shell for the internal dye. The proportional sensing strategy could overcome the concentration effect of nanoparticles due to the ratiometric response. Similar to rhodamine dyes, certain BODIPY dyes also exhibit temperature-dependent properties.

BODIPY-based fluorescent dyes respond to changes in temperature through the rotation of the phenyl group directly attached to the 8-position of the core (Fig. 2A).[33–35] Based on this property, the fluorescent temperature probes (3), reported by Kuimova et al., and (4), reported by Martí et al., which could serve as quantitative tools for intracellular temperature measurement.[36,37] In the case of probe 3, nonradiative relaxation accelerated as the temperature increased from 10 °C to 70 °C, leading to a significant decrease in both the fluorescence intensity and lifetime (Fig. 2B and C). Subsequent fluorescence intensity and lifetime imaging of U2OS cells containing probe 3 at variable temperatures from 11 °C to 37 °C revealed a similar temperature-dependent change (Fig. 2E).

It is crucial to acknowledge that the rotational properties of the phenyl group are also influenced by changes in viscosity, where an increase in viscosity suppresses the rotational freedom of the phenyl ring. As viscosity is dynamic in living cells, so shielding the effect of viscosity on fluorescence is critical. For example, in the case of probes 3 and 4, strategic modifications were introduced to counteract viscosity effects. Probe 3 incorporated cyclopropane substituents at the α-position, while probe 4 featured methyl groups at positions 1 and 7 of the BODIPY core. The specific modifications were designed to increase the energy barrier of phenyl rotation by introducing spatial resistance. These structural alterations create a scenario where the driving force provided by viscosity changes cannot reach the rotational energy barrier. As a result, the temperature measurements are shielded from the effects of viscosity changes. Probe 3 showed the weakest viscosity dependence when comparing it with the probe incorporating cyclopropane substituents at the β-position and the unmodified probe. Due to
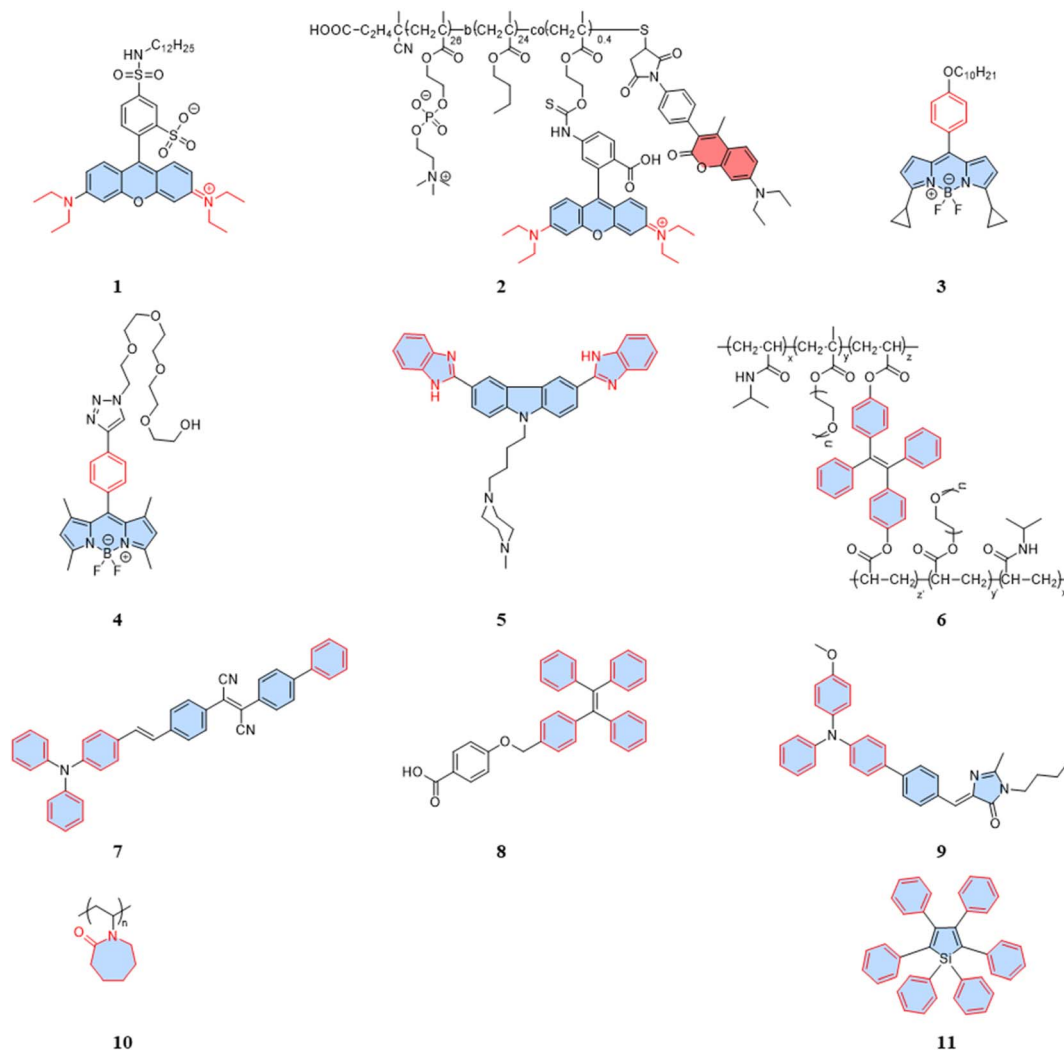
Fig. 1 Structures of intramolecular-rotation-based temperature probes.

its very low sensitivity to viscosity (Fig. 2D), probe **3** can be used as a temperature sensor, at least in nonpolar solvents. This also opens up the possibility for it to detect cell temperature. Furthermore, in the case of probe **4**, polyethylene glycol (PEG) modification was implemented to enhance the probe's water solubility and cell permeability. These adjustments in intramolecular rotational properties, influenced by different dyes, can be correlated with temperature. Similarly, AIE dyes also have limitations for the detection of intracellular temperature.

As is well known, for AIE dyes, intramolecular rotation is often associated with the states of aggregation and dispersion. AIE dyes are non-emissive in good solvents (dispersion state) but emit intensively as aggregates in poor solvents.[38] For conventional AIE dyes, their small molecular size often makes them have excellent intracellular dispersion, and difficult to aggregate (Fig. 3A). As a result, unmodified AIE dyes do not exhibit temperature-dependent changes in fluorescence, and fluorescence may not even be observed in cells.[38] To date, four approaches have been employed in utilizing AIE dyes for the development of fluorescent temperature sensing:

(i) Amphiphilic modification (Fig. 3B): this method involves modifying AIE dyes into amphiphilic molecules. The degree of aggregation of amphiphilic molecules in water depends on temperature. At low temperatures, the highly aggregated state restricts intramolecular rotation, leading to an increase in the fluorescence intensity. In contrast, at high temperatures, the mildly aggregated state leads to a decrease in fluorescence intensity. For instance, the fluorescent temperature probe (**5**), reported by Dey *et al.*, incorporates carbazole-based amphiphilic molecules that can form nanoparticles in aqueous media at low temperatures.[39] As the temperature increases, the probe undergoes a transition from aggregates to monomers, and the rotational acceleration of piperazines leads to a decrease in fluorescence intensity. For a fluorescent temperature probe (**6**), Tang *et al.* introduced a more hydrophilic oligo (ethylene glycol) methacrylate (OEGMA) into the polymer to finely adjust the hydrophilicity of the polymer.[40] By adjusting the hydrophilicity of the polymer, the phase-transition temperature could be precisely controlled within the physiological temperature range. The fluorescence intensity of each cycle was recorded at 43 °C
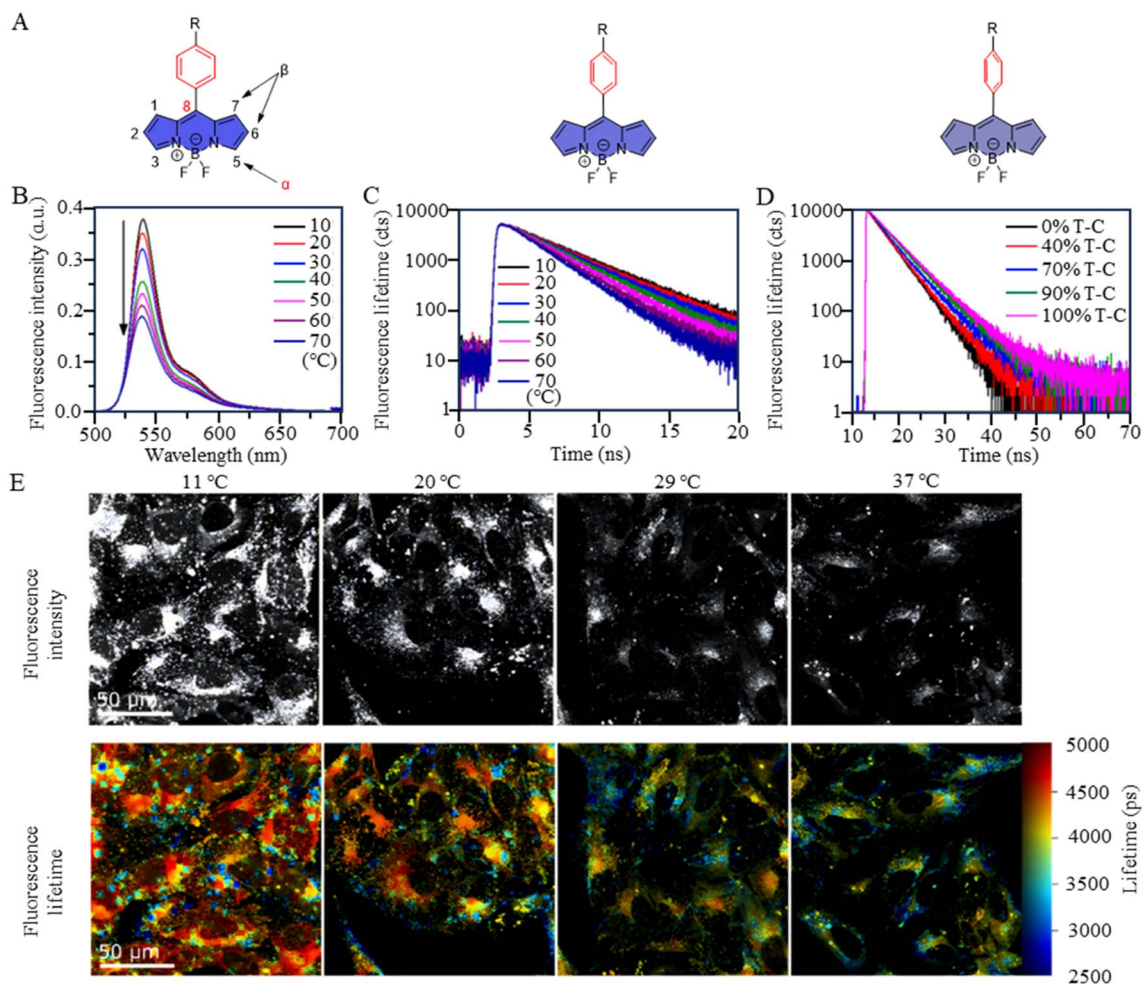
Fig. 2 (A) Temperature-response strategy of BODIPY-based dyes. (B) Fluorescence spectra of probe **3** at temperatures from 10 °C to 70 °C. (C) Fluorescence decays of probe **3** at temperatures from 10 °C to 70 °C in toluene. (D) Fluorescence decays of probe **3** in toluene–castor oil mixtures of different viscosities. (E) Fluorescent images of probe **3** in U2OS cells at variable temperatures between 11 °C and 37 °C.

and 33 °C, as shown in Fig. 3F, showing good consistency. Above the phase-transition temperature, the polymer contracted to form dense nanoparticles, inducing an RIR effect of tetraphenylethene (TPE) dyes.

(ii) Encapsulation (Fig. 3C): the second method involves encapsulating AIE dyes within nanoparticles, ensuring that the temperature-response process of the probe occurs inside the particles. By maintaining a uniform dispersion of nanoparticles, this method overcomes the drawbacks associated with AIE dyes, allowing for monitoring of particles' fluorescence. For instance, within the nanoparticles formed from the encapsulated matrix F127, the fluorescent temperature probe **7**, reported by Tian *et al.*, demonstrated an increase in nonradiative attenuation with increasing temperature.[41] The rotation of the benzene ring in this process depended on the molecular aggregation state within the nanoparticles, which was associated with the temperature change. As is shown in Fig. 3G, the fluorescent intensity ratios of the probe showed no significant change from 25 °C to 65 °C, indicating its good stability.

(iii) Thermoresponsive polymer incorporation (Fig. 3D): the third method involves introducing AIE dyes into

a thermoresponsive polymer, where changes in temperature change cause a shrinkage or expansion effect. The phase transition of the polymer causes a relative change in the spatial position of dyes. For instance, Zhang *et al.* reported a fluorescent temperature probe (**8**) attached to elastin-like polypeptides (ELPs40).[42] The shrinkage of ELPs40 at high temperature induced probe aggregation, leading to enhanced fluorescence of the internal TPE-derivative dyes. The results from heating–cooling cycles (25–50 °C) of ELPs40 containing probe 8 showed its reversibility (Fig. 3H). The repeatability of a probe's temperature response is correlated with its resistance to photobleaching. Photobleaching, which refers to the permanent loss of fluorescence after prolonged light exposure, is a major factor that affects the stability of fluorescent probes.[43] In general, a more stable molecular structure leads to a greater resistance to photobleaching and a more repeatable temperature response. Therefore, the stability of the molecular structure is crucial for minimizing photobleaching and ensuring a reliable temperature response. Similarly, saturated fatty acid chains, which are natural phase-change materials, have a distinct melting point. Tang *et al.* combined *in situ* surface
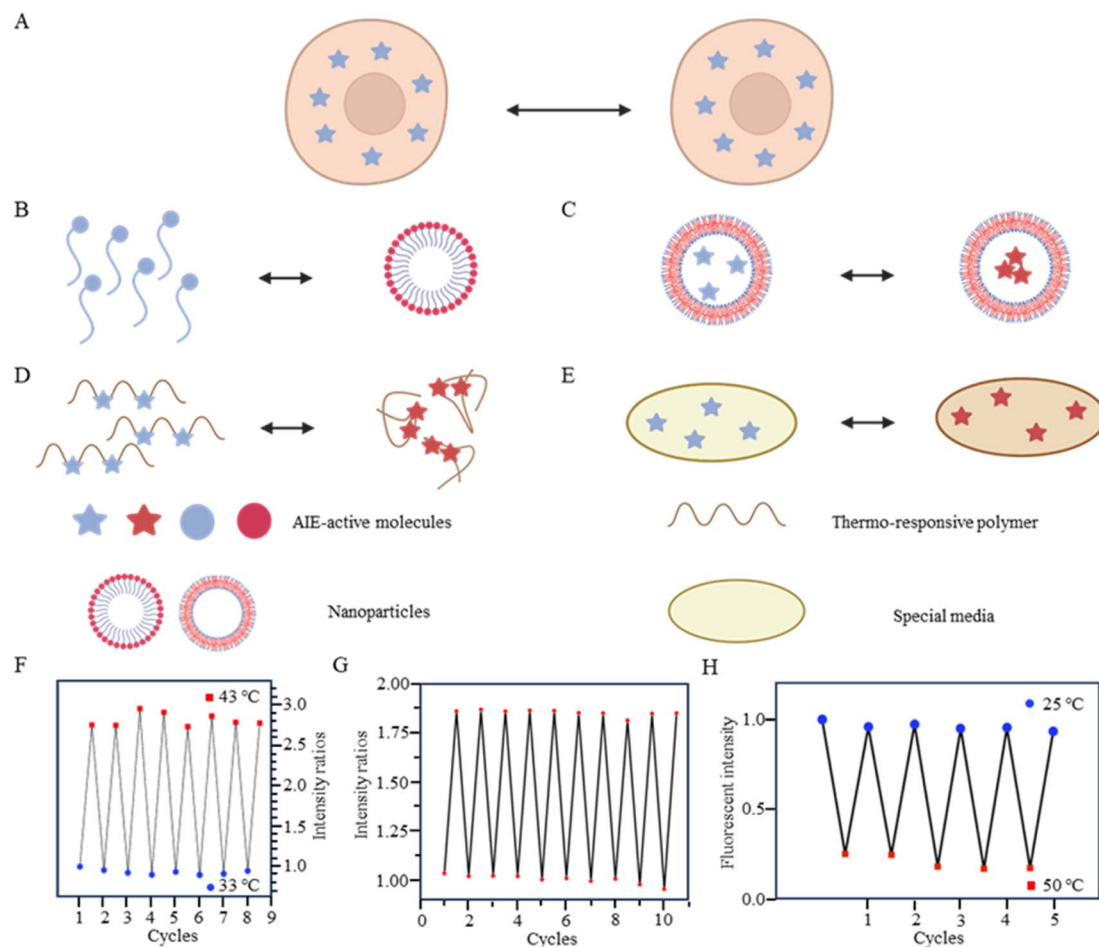
Fig. 3 (A) Temperature-response strategy of unmodified AIE dyes. (B) Temperature-response strategy combining amphiphilic molecules and AIE dyes. (C) Temperature-response strategy for nanoparticle-encapsulated AIE dyes. (D) Temperature-response strategy combining thermoresponsive polymers and AIE dyes. (E) Temperature-response strategy combining special media and AIE dyes. (F) Repeatability testing of probe **6**. (G) Repeatability testing of probe **7**. (H) Repeatability testing of probe **8**.

polymerization and nanoprecipitation to prepare nanoparticles containing probe **9** and natural saturated fatty acids.[44] The donor–acceptor (D–A) structure of the probe conferred it with a twisted intramolecular charge transfer (TICT) property. Thus, temperature sensing arose from the combined effect of its AIE and TICT properties. Specifically, when the temperature decreased, the fluorescent temperature probe exhibited a red-shifted emission, decreased fluorescence intensity, and elongated fluorescence lifetime. Conversely, when the temperature increased, the probe showed a blue-shifted emission, increased fluorescence intensity, and shortened fluorescence lifetime. Furthermore, electron-rich heteroatoms, such as nitrogen and oxygen, have been found could transform into unconventional luminophores when aggregated or clustered.[45] On this basis, De *et al.* designed a fluorescent temperature probe (**10**) based on electron-rich heteroatoms (O and N).[46] The combination of the temperature-driven aggregation behavior and AIE dyes enabled probe **10** to demonstrate a temperature response.

(iv) Special media-induced environmental changes (Fig. 3E): the fourth method involves inducing environmental changes in response to temperature through special media. For example,

Chen *et al.* designed a fluorescent temperature probe (**11**) combining hexaphenyl-1*H*-silole (an AIE dye) with a special matrix butter.[47] The viscosity of the butter decreased with increasing temperature, resulting in faster benzene ring rotation and a subsequent decrease in fluorescence intensity.

2.2 Polarity-sensitivity-based temperature probes

Indeed, a variety of well-developed polarity-sensitive fluorescent dyes are available.[48] The crucial aspect of employing these dyes for temperature sensing is to create a spatial environment where the polarity can be correlated to the temperature. Thermoresponsive polymers with hydration capabilities naturally meet these crucial requirements. Temperature changes induce alterations in the spatial conformation of such polymers, coupled with hydration and dehydration.[49] According to existing reports of intracellular fluorescent temperature probes, *N*-isopropylacrylamide (NIPAM) is the most commonly used such thermoresponsive polymer. With a low critical solution temperature (LCST) of 32 °C,[50] NIPAM undergoes a phase transition within the physiological temperature range. At lower

temperatures, the polymer assumes an extended structure with a significant number of water molecules, causing quenching of the surrounding polarity-sensitive fluorescent dyes. Conversely, at higher temperatures, the polymer transforms into a spherical conformation, expelling water molecules. This transition forms an apolar hydrophobic region within the polymer, enhancing the fluorescence of the polarity-sensitive fluorescent dyes. The spherical structure also minimizes the impact of intracellular polarity changes on the probes, particularly in cases of abnormal physiological functions. Therefore, the primary design strategy for such fluorescent temperature probes involves the combination of thermoresponsive polymers and polarity-sensitive fluorescent dyes.

In 2009, Uchiyama et al. reported a nanogel temperature probe that combined NIPAM with a polarity-sensitive dye.[51] The incorporation of fluorescent dyes into nanogels eliminated fluorescence enhancement/bursting caused by chemical interactions between the cellular components and fluorescent dyes. This study demonstrated the first instance where the

combination of a polarity-sensitive dye and a thermoresponsive polymer could detect intracellular temperature changes. Based on NIPAM, various fluorescent temperature probes (12, Guo et al.;[52] 13, Qi et al.;[53] 14, Qian et al.;[54] and 15, Yang et al.)[55] have been developed by incorporating 3-phenylamino substituted BODIPY, curcumins, and A1 and A2 dyes, respectively, where A1 consists of 2-(6-(4-(2-hydroxyethyl)piperazin-1-yl)-1,3-dioxo-1H-benzo[de] isoquin-olin-2(3H)yl)ethyl methacrylate, while A2 consists of dipyren-1-yl(2,4,6triisopropylphenyl) borane.

In addition, 7-nitro-1,2,3-benzoxadiazole (NBD), as an environmentally sensitive fluorescent dye, is often used as a sensor for polarity, pH, and specialized molecules.[56–58] Qi et al. (2014) developed a fluorescent temperature probe (16) composed of two polymer chains by incorporating a polarity-sensitive fluorescent dye (4-(2-acryloylaminoethylamino)-7-nitro-2,1,3-benzoxadiazole, NBDAA) and a polarity-insensitive fluorescent dye (a derivative of rhodamine B, RhBAM) into NIPAM, respectively (Fig. 4).[59] First, the polarity sensitivity of NBDAA was attributed to its interaction with water molecules, forming
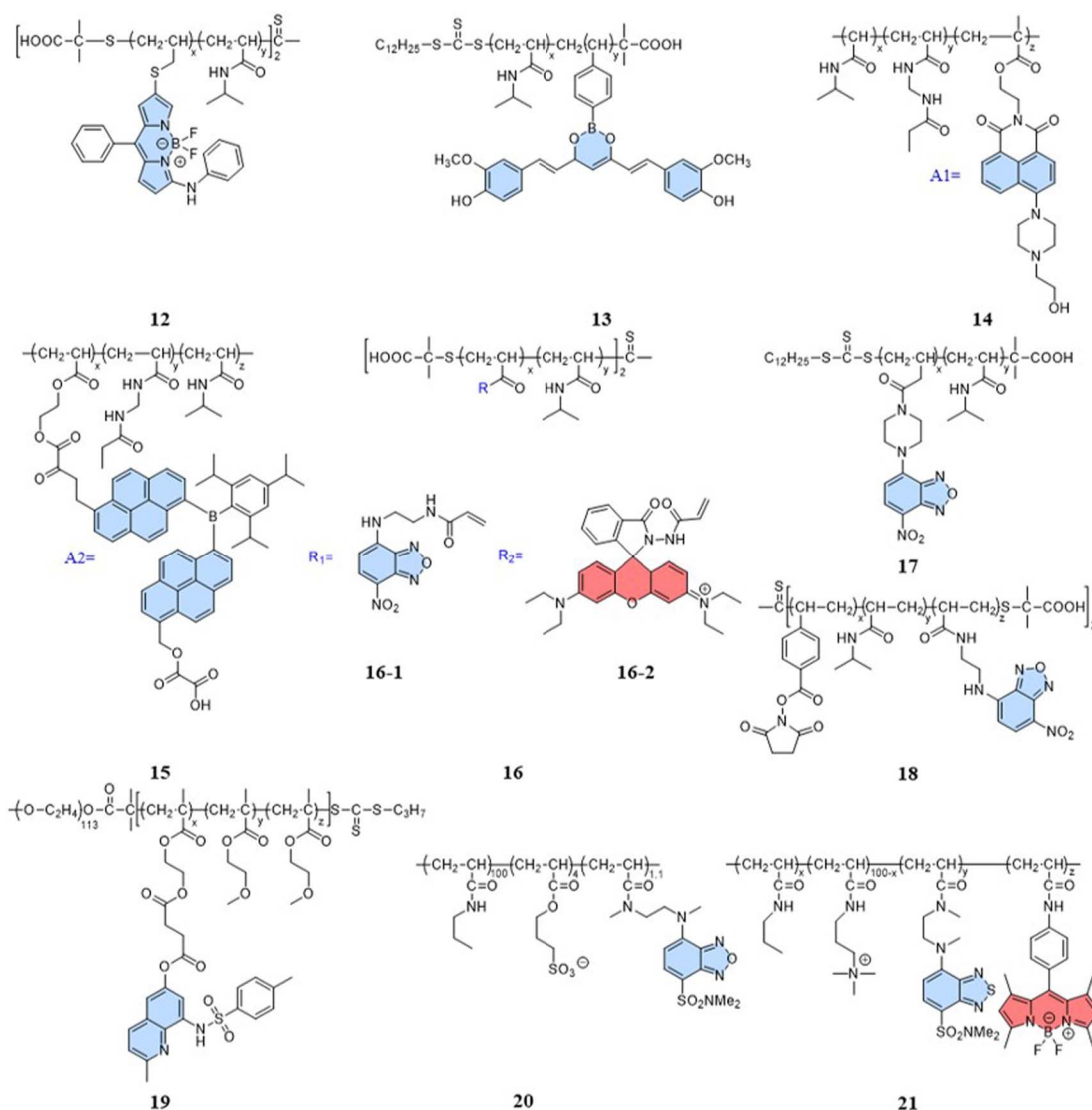

Fig. 4 Structures of polarity–sensitivity-based temperature probes.

intermolecular hydrogen bonds. This interaction resulted in the loss of excited state energy of the probe and a consequent decrease in its fluorescence intensity. Second, the design with two polymer chains was primarily aimed at preventing the significant effective energy transfer from NBDAA to RhBAM, ensuring that it did not impact the polarity-sensitive fluorescence changes (Fig. 5A). The fluorescence intensity of NBDAA at 530 nm exhibited a notable increase as the temperature rose, while the fluorescence intensity of RhBAM at 571 nm exhibited only slight changes (Fig. 5B). This phenomenon could be attributed to the spectral overlap between RhBAM and NBDAA, resulting in a slight increase in intensity at 571 nm with

increasing temperature. However, since the temperature sensing was obtained from the ratio of the two fluorescence intensities, it did not interfere with the ratio measurement. Ultimately, the intensity ratio ($I_{530\ nm}/I_{571\ nm}$) was enhanced with increasing temperature (Fig. 5C). Intracellular temperature imaging in HeLa cells revealed that the emission fluorescence intensity of **16-1** channels increased, while the emission fluorescence intensity of **16-2** channels did not show observable changes from 33.3 °C to 39.2 °C. Ultimately, the color of the ratio channel changed from red to green with the temperature (correlation coefficient of 0.945) (Fig. 5D). The polarity-sensitive properties of NBD dyes and the thermoresponsive properties of
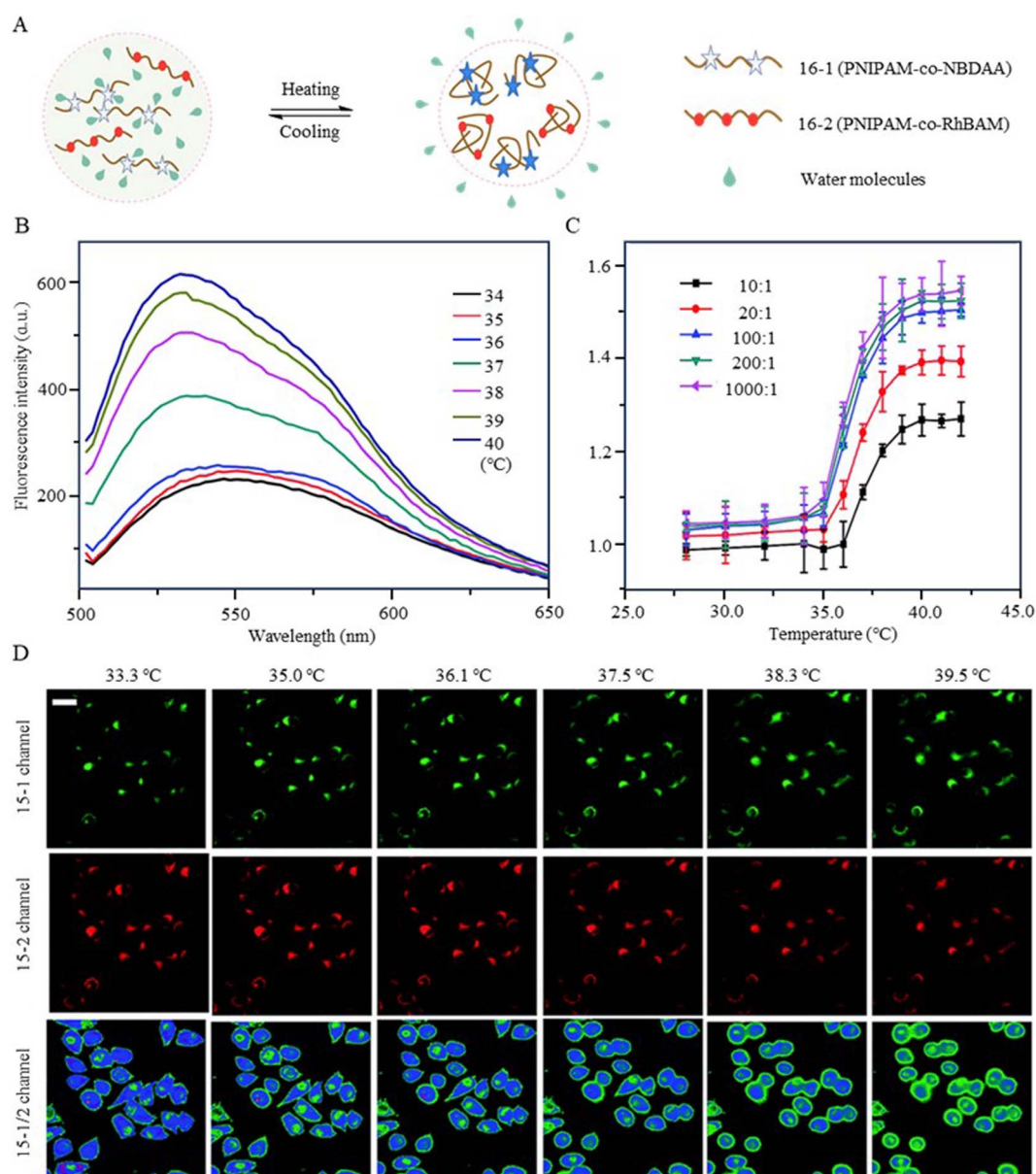

Fig. 5 (A) Temperature-response strategy of the fluorescent temperature probe **16**. (B) Fluorescence spectra of the probe at temperatures from 34 °C to 40 °C. (C) Temperature-responsive calibration plot of the probe. The probe was composed of **16-1/16-2** (100 : 1). (D) Fluorescent images of HeLa cells at different temperatures 33.3 °C, 35.0 °C, 36.1 °C, 37.5 °C, 38.3 °C, and 39.2 °C, respectively. The images of the first row (**16-1** channel) and the second row (**16-2** channel) were collected in the ranges 510–560 nm and 570–670 nm, respectively. The images of the third row show the ratio channels.

NIPAM also enabled the fluorescent temperature probes **17** and **18** to achieve a response to intracellular temperature (Fig. 4).[60,61] All the probes exhibited notable alterations in fluorescence intensity when subjected to cellular temperatures exceeding 32 °C. Therefore, the LCST of thermoresponsive polymers determines the applicable temperature range of the fluorescent temperature probes. Only when the actual temperature exceeds this value, will significant fluorescence changes accompanied by localized polarity changes be observed.

Considering the limitation of the LCST of NIPAM for its temperature detection range, it is essential to design and synthesize thermoresponsive polymers with a lower LCST. This can aid studying changes in physiological functional states at low temperatures. Liu *et al.* reported a fluorescent temperature probe (**19**) based on an amphiphilic block copolymer.[62] The LCST of the thermoresponsive polymer could be adjusted by changing the ratio of the molar contents of OEGMA. Ultimately, the probe could produce a temperature response in the range of 26–42 °C. Next, Uchiyama *et al.* developed a fluorescent temperature probe (**20**) using poly-*N-n*-propylacrylamide (NNPAM) as a thermoresponsive polymer, which could detect temperature changes within the range of 20–50 °C.[63] On this basis, they synthesized a ratiometric fluorescent temperature probe (**21**) by adding a BODIPY-based dye and a cationic unit.[64] The cationic unit was able to introduce the probe spontaneously into the cell and prevented aggregation between the probes. This property reduced the bias caused by an uneven dispersion of the probe distribution.

2.3 FRET-based temperature probes

The utilization of the FRET mechanism has led to the development of a diverse range of ratiometric fluorescent probes for intracellular detection.[65,66] These probes are often used in intracellular assays, especially for assessing intracellular states and active processes.[67] Establishing the FRET mechanism requires at least two fluorescent dyes. However, this introduces the potential for interference arising from the microenvironment changes. Therefore, the development of fluorescent temperature probes that respond to intracellular temperature changes using the FRET mechanism is more challenging.

Currently, the primary design strategy for this type of fluorescent temperature probe is to introduce at least one dye from FRET pairs into a thermoresponsive polymer. Conformational changes (extension and shrinkage) in the dye-labeled polymer chains alter the spatial distances of the FRET pairs. Thus, the efficiency of FRET between a donor and acceptor can produce temperature-dependent ratiometric changes. Notably, the dyes used to construct FRETs often do not appear on the same polymer. When two or more fluorescent dyes are located on the same polymer, the FRET efficiency between them is substantial enough. This can lead to an insignificant FRET efficiency caused by phase transitions in the polymer, resulting in a lower temperature resolution.

Zhang *et al.* (2018) designed a fluorescent temperature probe (**22-1/2**) consisting of a mixture of the NIPAM-based fluorescent dye **22-1** and *N*-isopropylmethacrylamide (NIPmAM)-based fluorescent dye **22-2** (Fig. 6).[68] The incorporation of the methyl group
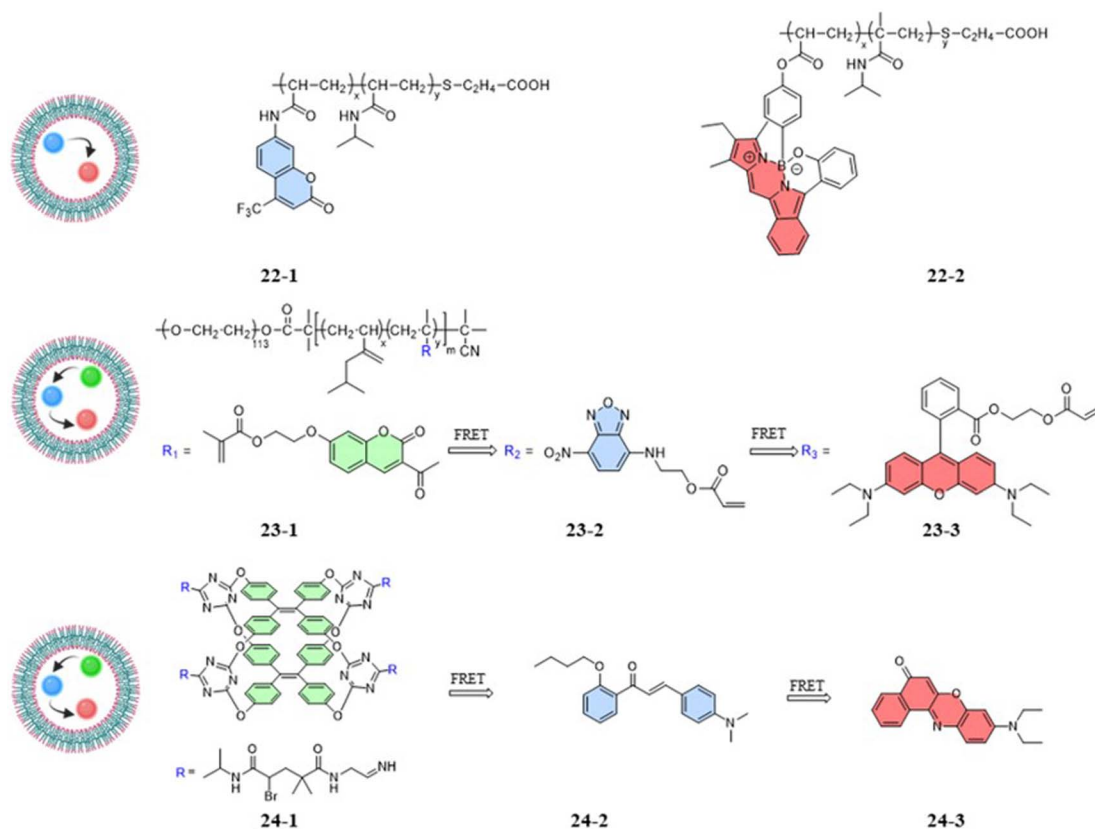

Fig. 6 Structures of FRET-based temperature probes.

resulted in a higher LCST for NIPmAM (48.6 °C) relative to NIPAM (31.1 °C). Thus, the two polymer chains shrank and extended at different rates with temperature (Fig. 7A). This variability caused the probe to be able to continuously vary the FRET efficiency over a wide temperature range of 25–50 °C. With increasing the temperature, the fluorescence at 628 nm was enhanced, while the fluorescence intensity at 436 nm was decreased significantly (Fig. 7B). Additionally, there was a linear relationship (correlation coefficient of 0.96) between the fluorescence intensity ratio $I_{628\ nm}/I_{436\ nm}$ and temperature (Fig. 7C). Probes **22-1** and **22-2**

showed cellular imaging in blue and red, respectively (Fig. 7D). The fluorescence images of HeLa cells carrying the probe showed changes at 25 °C and 37 °C with a decrease in the blue fluorescence intensity and an increase in the red fluorescence intensity. As a result, the **22-1/2** channel showed enhanced fluorescence (Fig. 7E). This study demonstrated that probes based on one-step FRET could achieve an intracellular temperature response through the efficiency of FRET.

Compared to one-step FRET, the design of a two-step cascade FRET can achieve effective long-range energy transfer,
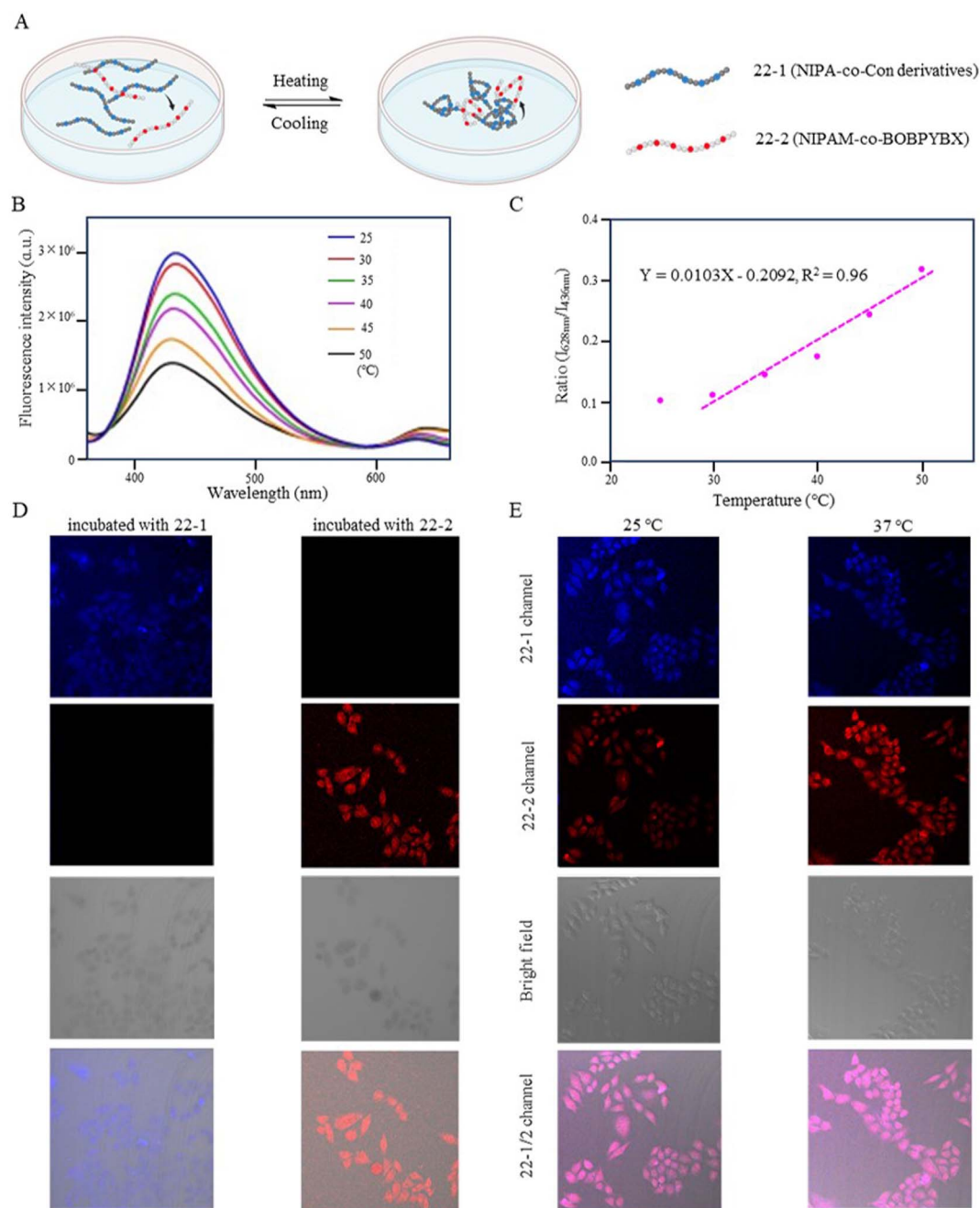

Fig. 7   (A) Temperature-response strategy of the fluorescent temperature probe **22-1/2**. (B) Fluorescence spectra of the probe at temperatures from 25 °C to 50 °C. (C) Linear correlation of the probe between the emission intensity ($I_{628\ nm}/I_{436\ nm}$) and temperature. (D) Fluorescent images of HeLa cells incubated with the probes **22-1** and **22-2**. (E) Fluorescent images of HeLa cells incubated with the probe **22-1/2** at 25 °C and 37 °C.

a significant Stokes shift, and a controllable fluorescence color. As shown in Fig. 6, the fluorescent temperature probes **23-1/2/3** and **24-1/2/3** achieved temperature responses by a two-step cascade FRET.[69,70] For probes **23-1/2/3** reported by Liu *et al.*, coumarin dye, 7-nitro-2,1,3-benzoxadiazole dye, and rhodamine B dye were copolymerized with NIPAM to form **23-1**, **23-2**, and **23-3**, respectively. Similarly, Tang *et al.* synthesized probes **24-1/2/3** using three different fluorescent dyes. The fluorescent dye **24-1** was based on the AIE dye TPE and NIPAM, while the fluorescent dye **24-2** was based on 4-dimethylamino-2′-butoxychalcone, and the fluorescent dye **24-3** was based on Nile Red. Different luminescence colors could be achieved by regulating the mass ratio of the three dyes. Since the probes had both thermoresponsive polymers and AIE TPE dyes, the temperature response had different strategies. The temperature-responsive processes mainly included process: (1) under LCST, whereby the nonradiative relaxation process generated by the rotation and vibration of the benzene ring dominated with increasing temperature. Through cascade FRET, the fluorescence intensity of all three dyes decreased; and (2) above LCST, whereby the shrinkage of the thermoresponsive polymer dominated with increasing temperature. Accompanied by a decrease in the distance between the three fluorescent dyes, the energy-transfer efficiency increased significantly. As a result, the probe was able to produce a reversible change of the probe from orange to white with a temperature resolution more significant than 0.5 °C.

3 Fluorescent thermometry of mitochondria

Diseased cells associated with mitochondrial dysfunction use temperature abnormalities as one of the signals. Mitochondria are at the crossroads of many cellular processes and play a crucial role in heat stress-induced apoptosis in certain cell lines.[71] It has been shown that external temperature induction leads to a positive stress response in brain and heart mitochondria.[72,73] Temperature can be central to abnormal mitochondrial function and functional regulation, and therefore, modulation by temperature may be an effective adjunctive therapy for mitochondrial diseases. However, the mechanism of the role of temperature in signaling pathways is still unclear. Fluorescent thermometry is beneficial for studying the process of biological responses or signaling in mitochondria. A potential problem, though, is that the changes in size and environment from the cell-sale to mitochondria may introduce more instability to temperature detection.

3.1 Intramolecular-rotation-based temperature probes

Research has shown that small nanoparticles and molecules can flow through the bloodstream and thus can be distributed along the target tissue after intravenous injection.[74] Chemical modifications and the addition of targeting units can enable the detection of target cells and organelles. However, mitochondria
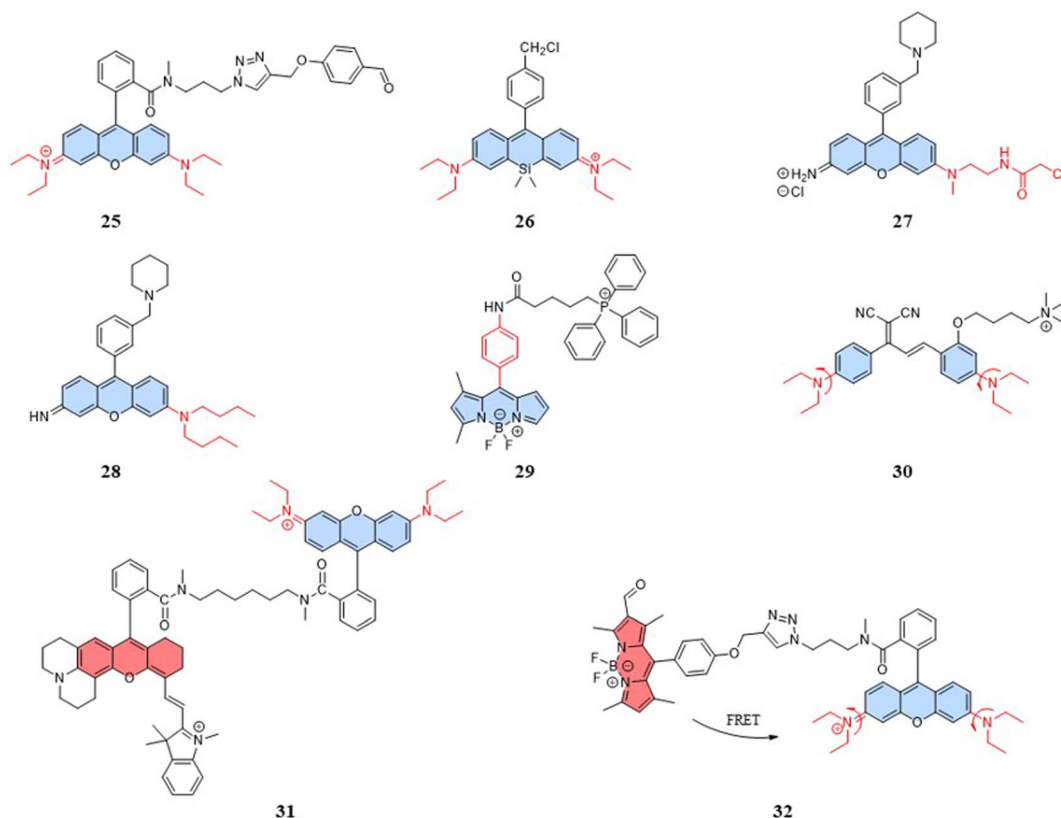

Fig. 8 Structures of intramolecular-rotation-based temperature probes.

present new challenges for designing fluorescent temperature probes due to their complex microenvironment, which includes targeting mechanisms and temperature resolution. For the choice of targeting mechanisms, two targeting mechanisms in mitochondria are: electrostatic binding related to membrane potential and covalent binding related to membrane proteins. The fluorescent temperature probes **25–27** formed strong covalent bonds with membrane proteins *via* benzaldehyde, chloromethyl, and chloroacetyl motifs, respectively (Fig. 8).[75–77] Both binding mechanisms have advantages and disadvantages. The former has more binding sites, but physical binding results in probe instability. Also, changes in membrane potential caused by mitochondrial dysfunction inevitably lead to probe leakage. On the other hand, although covalent binding can achieve the permanent immobilization of probes, the choice of targeting groups and the complexity of membrane proteins make the design of the probes more challenge. In-depth studies of mitochondrial membranes and the continuous exploration of targeting groups aim to provide more selectivity for the covalent binding of probes. To address the challenge of light penetration in tissue studies, high fluorescence penetration is essential. This is often achieved by the design and modification of fluorescent dyes. For example, replacing the O atom in the heteroanthracene fraction with a Si atom gave probe **26** reported by Guo *et al.* strong near-infrared (NIR) fluorescence properties, which also increased the light penetration of the probe in tissue sample detection.

In addition to mitochondrial binding, the temperature resolution of the probes plays a crucial role in determining whether it can be used for the real-time dynamic monitoring of mitochondria. Physiological processes that are associated with temperature variations of ∼1 °C have been reported that demand a finer temperature resolution to accurately monitor certain diseases, ideally lowering the current 0.5 °C to 0.1 °C.[19] For intramolecular-rotation-based temperature probes, the temperature resolution depends on the degree of rotational freedom. Both the fluorescent temperature probes **27**,[77] reported by Rak *et al.*, and **28**,[78] reported by Chang *et al.*, showed increased rotational freedom of the thermosensitive units by replacing the ethylamino group with a substituent with a larger rotational radius. Moreover, Chang *et al.* reported a fluorescent temperature probe (**29**) based on an asymmetric BODIPY-based dye.[79] The asymmetric structure made the benzene ring rotate with a lower energy barrier, thereby increasing the probe's temperature-dependent rotational freedom. We can find that most of the probes for mitochondrial temperature detection are based on rhodamine and BODIPY dyes. Therefore, there is an urgent need to explore new thermosensitive dyes.

With the study of temperature-dependent rotational groups, probes combining different functional groups can provide more options for achieving fluorescent temperature probes. Hu *et al.* (2022) synthesized a fluorescent temperature probe (**30**) by combining diethylamine groups, a mitochondrion-targeting moiety (a positive quaternary ammonium salt), and a designed fluorescent moiety (Fig. 8).[80] The probe demonstrated high sensitivity and NIR emission (600–670 nm). The fluorescence intensity at 660 nm was increased by approximately 28-fold as the temperature decreased from 60 °C to 25 °C (Fig. 9A). Mitochondria were targeted by the probe in para-cancerous tissue (control) and human liver tumor cells. The
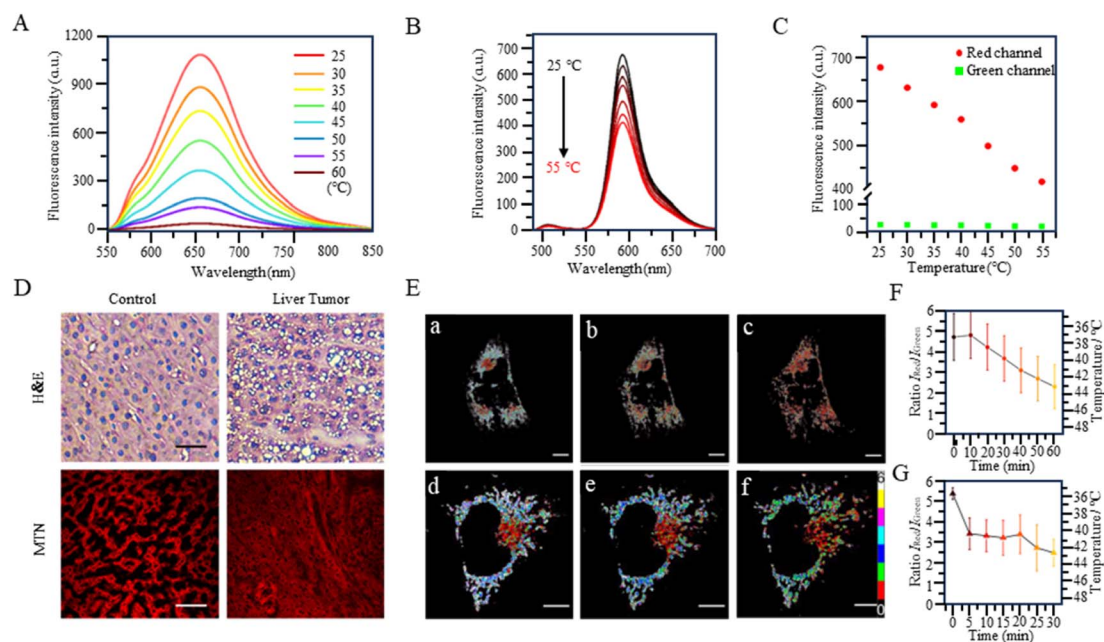

Fig. 9 (A) Fluorescence spectra of fluorescent temperature probe **30** at temperatures from 25 °C to 60 °C. (B) Fluorescence spectra of fluorescent temperature probe **32** at temperatures from 25 °C to 50 °C. (C) Fluorescence intensity of the two emission maxima. (D) H&E and histofluorescence imaging of human hepatocellular carcinoma tissues. (E) (a–c) Time course image of *S. aureus*-stimulated HeLa cells over 60 min. (d–f) Time course image of LPS-stimulated HeLa cells over 30 min. (F) Changes in the intensity ratio I_{Red}/I_{Green} in mitochondria in (a–c). (G) Changes in the intensity ratio I_{Red}/I_{Green} in mitochondria in (d–f).

results showed that the fluorescence in liver tumors was significantly weaker than in the control group, indicating an increase in mitochondrial temperature in liver tumors (Fig. 9D). Although changes in fluorescence intensity by a single-wavelength-based probe can provide evidence of temperature anomalies, the deviations from the probe concentration may limit accurate temperature measurements.

The fluorescent temperature probes 31 (ref. 81) and 32 (ref. 14) were designed to minimize the effects of the probe concentration by using a ratiometric response. Ultimately, both probes achieved temperature sensitivities of 2.65% $°C^{-1}$ and 5.4% $°C^{-1}$, respectively. Probe 31 reported by Takeoka *et al.* was composed of two kinds of rhodamine dyes: a temperature-sensitive rhodamine B dye and a temperature-insensitive CS NIR dye. Their excitation wavelengths were 563 and 722 nm, respectively. In contrast to the dual light source excitation requirement for probe 31, the FRET-based probe 32, as reported by Xiao *et al.*, achieved proportional temperature detection with a single light source excitation through FRET from BODIPY to rhodamine dye. This design effectively avoided the signal interference that multiple light sources may introduce. Also, the fluorescence intensity of probe 32 decreased with increasing temperature, establishing an excellent linear correlation ($R = 0.99$) between the intensity ratio (I_{Red}/I_{Green}) and temperature

(Fig. 9B and C). As shown in Fig. 9E, the mitochondrial temperature was visualized in live HeLa cells in an inflammatory state using probe 32. Following *S. aureus* stimulation, cells showed a slight decrease in the two-channel fluorescence ratio over 60 min, indicating a slow and sustained increase in mitochondrial temperature from 38 °C to 43 °C (Fig. 9Ea–c and F). In LPS-treated inflammatory cells, the mitochondrial temperature increased by 4 °C immediately within the first 5 min and then progressively increased by 2 °C after a further 20 min (Fig. 9Ed–f and G). This study demonstrated the increase in mitochondrial temperature in inflammatory cells.

3.2 Structural-changes-based temperature probes

The photophysical properties of fluorescent dyes, including factors such as the absorption and emission wavelengths, quantum yield, and fluorescence intensity, are closely related to their molecular structures. In the case of rhodamine dyes, their fluorescent characteristics depend on the xanthene moiety. Disruption of the conjugated structure of the xanthene induces changes in the fluorescence. The fluorescent temperature probes 33,[82] reported by Bai *et al.*, and 34,[83] reported by Kang *et al.*, enabled the detection of mitochondrial temperature by utilizing the conversion between the fluorescent and non-fluorescent states of rhodamine dyes (Fig. 10A). Taking probe
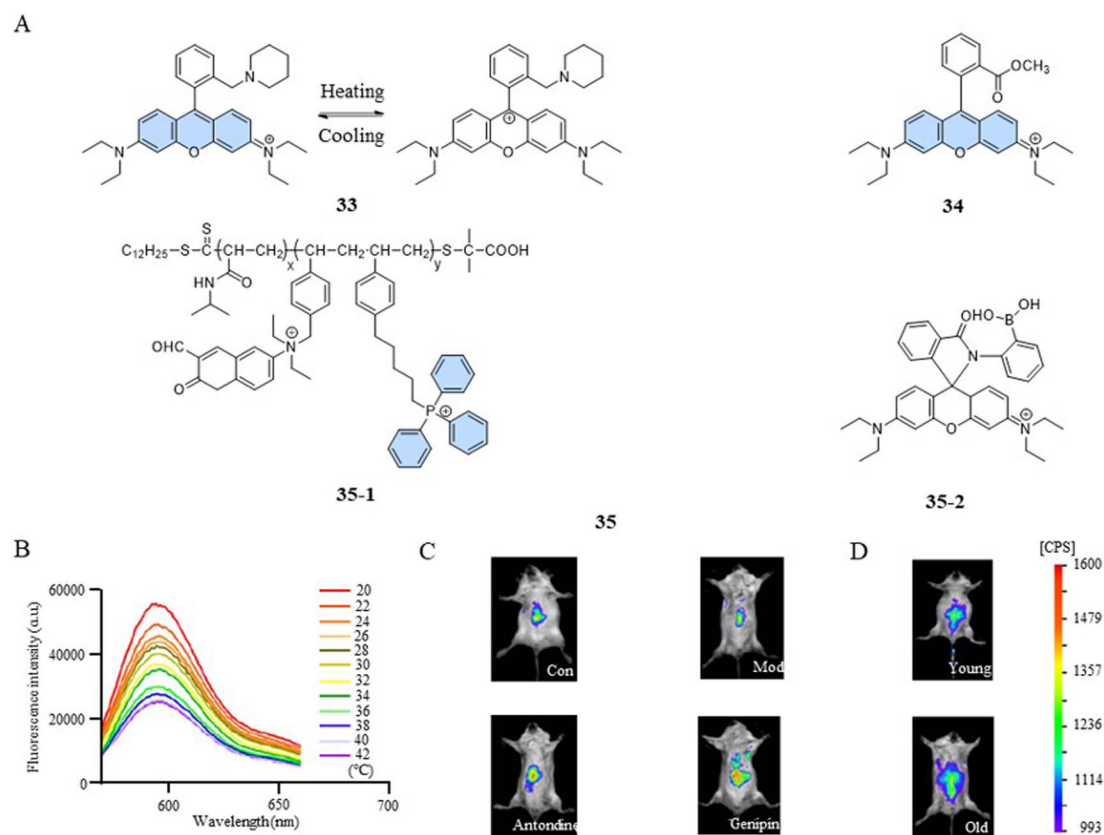

Fig. 10 (A) Structures of structural-change-based and polarity-sensitivity-based temperature probes. (B) Fluorescence spectra of fluorescent temperature probe 33 at temperatures from 20 °C to 42 °C. (C) 2,4-Dinitrophenol (28 mg kg^{-1}) was used to induce fever in mice (mod), and the antipyretic drugs antondine (20 mg kg^{-1}) and genipin (50 mg kg^{-1}) were administered to treat fever. (D) Fluorescent images of young and old mice.
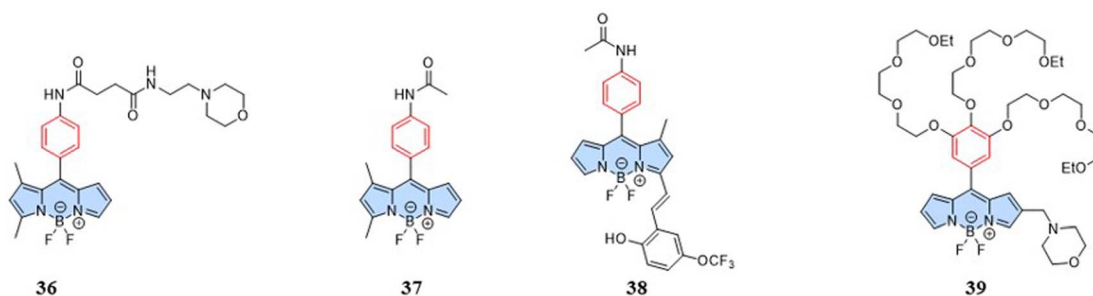
Fig. 11 Structures of intramolecular-rotation-based temperature probes.

33 as an example, at lower temperatures, the probe was more likely to form unstable ion pair forms under the control of kinetic factors, exhibiting strong fluorescence. With the increase in temperature, the ion pairs were disrupted or partially broken, transitioning into a symmetrical non-fluorescent form. The fluorescence intensity of the probe exhibited a decrease with increasing temperature within the range of 20–42 °C (about 3.92% °C^{-1}) (Fig. 10B). In comparison to the control group, 2,4-dinitrophenol-induced mice exhibited a low fluorescence intensity. However, subsequent treatment with antondine or genipin resulted in an enhancement in fluorescence intensity and a reduction in the mice body temperature (Fig. 10C). As shown in Fig. 10D, older mice exhibited more fluorescence and lower body temperatures compared to their younger counterparts. This study demonstrated that structural changes in fluorescent dyes can obtain a responsive capability to changes in mitochondrial temperature.

However, a single temperature assay can only reveal mitochondrial temperature abnormalities. To gain a deeper understanding of the relationship between mitochondrial dysfunction and temperature variations, a versatile fluorescent probe becomes indispensable. Such a probe should have the ability to detect both the functional state and temperature changes within mitochondria simultaneously. Qi et al. reported a fluorescent temperature probe (**35**) that could simultaneously detect mitochondrial temperature and ATP fluctuations.[16] The thermoresponsive unit of the fluorescent dye **35-1** underwent a transition from hydrophilic to hydrophobic as the temperature increased, resulting in a polarity-sensitive temperature response. Meanwhile, the fluorescent dye **35-2** detected changes in ATP levels through an open- or closed-loop fluorescence switching mechanism. This study showed that during oxidative phosphorylation, the release of energy led to both an increase in mitochondrial temperature and a decrease in ATP levels.

4 Fluorescent thermometry of other organelles

In addition to mitochondria, the endoplasmic reticulum (ER) and lysosomes play important roles in maintaining intracellular homeostasis. ER is an essential organelle for protein and lipid synthesis in hepatocytes.[84] ER stress can disrupt hepatic energy metabolism, potentially resulting in metabolic disorders, such as hepatic steatosis and hypoglycemia.[85] Lysosome acts as a control center for catabolic and anabolic processes, maintaining cellular energy homeostasis.[86] Thus, the temperature of the ER and lysosomes is critical for maintaining biological system homeostasis. Fluorescent temperature probes (**36**, targeting lysosomes),[79] (**37**, targeting ER),[79] and (**38**, targeting ER)[87] have been used to achieve suborganelle temperature responses through fluorescence changes associated with rotation of the benzene ring. Additionally, Kuang et al. (2014) reported a fluorescent temperature probe (**39**) based on BODIPY dyes for targeting lysosomes.[88] At high temperature, the thermo-dehydration of the triple oligoethylene glycol groups increased the microviscosity and hydrophobicity. Due to the increased microviscosity around the probe, the fluorescence intensity of the probe gradually increased with increasing temperature (Fig. 11).

5 Summary and outlook

The review provides a comprehensive overview of small-molecule- and polymer-based fluorescent temperature probes designed for sensing temperatures from the cellular scale to mitochondria. Based on the four temperature-response strategies, we further analyzed the chemical modifications and biological applications of the probes. However, external conditions, such as changes in viscosity and pH, are often the main contributors to inaccuracies in temperature measurement. This includes differences in the internal environment of cells and organelles within different tissues. As can be seen, temperature-specific response remains the biggest challenge for fluorescent temperature probes. In this context, the exploration of probes specifically designed for detecting mitochondrial temperature is deemed imperative for enhancing the accuracy in fluorescent measurements.

For small-molecule fluorescent temperature probes: (1) the temperature response based on intramolecular rotation is generated by a decrease in fluorescence intensity and lifetime with increasing temperature. At high temperatures, the background signal is more likely to interfere with the weak fluorescence signal of the probe, which is not conducive to probing the microscopic mechanism of elevated cell temperature. Therefore, it is necessary to design a "turn-on" type of fluorescent temperature probe, where the signal increases with

temperature. This approach could enhance the detection sensitivity and facilitate the microscopic examination of elevated cell temperature. (2) Mitochondrial temperature detection faces challenges due to the complex microenvironment. Factors such as changes in viscosity, pH, membrane potential, and ion concentrations may directly influence the electron transition probability of the molecules, leading to potential inaccuracies in temperature sensing. To address this, the rational design and encapsulation of nanoparticles can be effective strategies to attenuate the effects of the microenvironment, improving the accuracy of mitochondrial temperature measurements.

For polymer fluorescent temperature probes: (1) although polymers can protect internal fluorescent dyes, the large sizes of polymers can result in their uneven distribution within the cell. This uneven distribution may lead to localized fluorescence signal anomalies, potentially causing incorrect temperature detection values. To address this issue, the introduction of charged ionic units into the polymer can improve probe dispersion through electrostatic interactions. This approach aims to enhance the uniform distribution of the probes within cells. (2) At high temperatures, thermoresponsive polymers shrink, which may cause the internal fluorescent dyes to produce aggregation-caused fluorescence quenching. Therefore, the design of probes needs to consider the number of fluorescent dyes attached to the polymer chain and control the distance between each fluorescent dye. By carefully addressing these considerations in the probe design, researchers aim to improve the performance and reliability of polymer-based fluorescent temperature probes, especially under conditions of elevated temperature. (3) Due to the limitations of the LCST, few types of thermoresponsive polymers can be used for physiological temperatures. This significantly limits the ability of fluorescent temperature probes to modulate the detectable temperature range. The LCST of NIPAM-based polymers is associated with the hydrophilic groups within the molecule. Therefore, the more hydrophilic groups contained in the molecule, the stronger the hydrogen bonding and the higher the LCST. Methods to further broaden the thermoresponsive range of NIPAM-based polymers include: (1) Adjusting the monomer content. The NIPAM monomer contains a large number of amide hydrophilic groups, which contribute to the polymer's hydrophilicity. Therefore, adjusting the proportion of NIPAM can change the LCST of the polymer, thereby broadening the range of response;[89] (2) molecular design. The temperature-response range of the polymer can be adjusted by copolymerizing different hydrophilic monomers with NIPAM. Available monomers include the more hydrophilic regulatory oligo(ethylene glycol) methacrylate and the less hydrophilic methyl methacrylate.[90]

In the context of small-sized suborganelles, most fluorescent temperature probes are designed based on small molecules, probably because the thermal effect of polymer probes is difficult to ignore.[19] To advance the development of more effective fluorescent probes tailored for the detection of mitochondrial temperature, the following research directions can be considered: (1) Designs where the fluorescence intensity or lifetime of the probe has positive feedback on the mitochondrial temperature. In this type of design, the fluorescence intensity or lifetime increases with increasing temperature, providing an advantageous mechanism for shielding the background fluorescence signals and thereby enhancing the resolution of the probe; (2) reversible fluorescent temperature probes that could allow the real-time detection of temperature, whereas the irreversible fluorescent temperature probe can detect instantaneous temperatures. By establishing a threshold temperature for the fluorescence switch, it can provide early warnings of mitochondrial temperature abnormalities. Furthermore, this method simplifies the post-processing steps for the fluorescence signal; (3) super-resolution fluorescent probes that could provide higher temporal and spatial resolution for temperature detection. Super-resolution fluorescence microscopy could also enable a more accurate visualization of cells and organelle temperatures. The combination of super-resolution and temperature response is a promising area of exploration in the context of fluorescent temperature probes; (4) combination approaches. Apparently, multifunctional fluorescent temperature probes exhibit diverse functions contingent on the temperatures. It has been reported that fluorescent thermometers can serve as carriers for drugs, determining drug release based on temperature response.[91,92] Therefore, the combination of temperature response with photothermal or photodynamic therapy presents another avenue for exploration.

The advent of thermoresponsive dyes has significantly made intracellular temperature detection a fascinating field. This review seeks to provide readers with fundamental insights into the realm of fluorescent temperature probes. Through an analysis of the latest advancement in probe development, the review aims to inspire researchers to develop new and innovative probes with broad applicability across scientific and medical domains.

Author contributions

Conceptualization: Lin Li, Duoteng Zhang, Shiji Zhang, Shuai Li, Yaoxuan Li, investigation: Shuai Li, Yaoxuan Li, Shiji Zhang, Duoteng Zhang, project administration: Lin Li, Shiji Zhang, visualization: Shuai Li, Yaoxuan Li, Shiji Zhang, Duoteng Zhang, Haixiao Fang, Aixiang Ding, Lin Li, resources: Yaoxuan Li, Lin Li supervision: Lin Li writing – original draft preparation: Shuai Li writing – review & editing: Yaoxuan Li, Shiji Zhang, Duoteng Zhang, Ze Huang, Haixiao Fang, Aixiang Ding, Kajsa Uvdal, Zhangjun Hu, Kai Huang, Lin Li.

Conflicts of interest

There are no conflicts to declare.

Acknowledgements

References

1 P. Yu, W. Qi, B. Huwatibieke, J. Li, X. Wang and H. Cheng, *Arch. Biochem. Biophys.*, 2019, **666**, 8–15.

2 X. R. Tan, M. C. Stephenson, S. B. Alhadad, K. W. Loh, T. W. Soong, J. K. Lee, I. C. Low and J. Sport, *Health Sci.*, 2023, **12**, 1–10.

3 D. B. Reichling, P. G. Green and J. D. Levine, *Pain*, 2013, **154**, S2–S9.

4 R. Moreno-Loshuertos, J. Marco-Brualla, P. Meade, R. Soler-Agesta, J. A. Enriquez and P. Fernández-Silva, *Mitochondrion*, 2023, **69**, 83–94.

5 D. Macherel, F. Haraux, H. Guillou and O. Bourgeois, *Biochim. Biophys. Acta, Bioenerg.*, 2021, **1862**, 148348–148364.

6 A. M. Bertholet and Y. Kirichok, *Annu. Rev. Physiol.*, 2022, **84**, 381–407.

7 D. Sung, B. B. Risk, K. J. Wang, J. W. Allen and C. C. Fleischer, *J. Magn. Reson. Imaging*, 2023, **57**, 1222–1228.

8 R. Howard, A. Scheiner, J. Cunningham and R. Gatenby, *PLoS Comput. Biol.*, 2019, **15**, e1007372–e1007389.

9 Z. El-Gammal, M. A. Nasr, A. O. Elmehrath, R. A. Salah, S. M. Saad and N. El-Badri, *Pflug. Arch. Eur. J. Phy.*, 2022, **474**, 1043–1051.

10 A. Sidenkova, *Eur. Psychiatry*, 2023, **66**, S100–S101.

11 M. Rango, A. Arighi, C. Bonifati, R. Del Bo, G. Comi and N. Bresolin, *J. Cereb. Blood Flow Metab.*, 2014, **34**, 915–920.

12 H. L. Chen, K. Yamada, K. Sakai, C. H. Lu, M. H. Chen and W. C. Lin, *Neurol. Sci.*, 2020, **41**, 1267–1276.

13 L. Ruan, J. Chen, C. Du, H. Lu, J. Zhang, X. Cai, R. Dou, W. Lin, Z. Chai, G. J. Nie and Y. Hu, *Bioact. Mater.*, 2022, **13**, 191–199.

14 Z. Huang, N. Li, X. Zhang and Y. Xiao, *Anal. Chem.*, 2021, **93**, 5081–5088.

15 T. Matsukawa, M. Ozaki, T. Nishiyama, M. Imamura and T. Kumazawa, *Crit. Care Med.*, 2000, **28**, 532–536.

16 J. Qiao, C. Chen, D. Shangguan, X. Mu, S. Wang, L. Jiang and L. Qi, *Anal. Chem.*, 2018, **90**, 12553–12558.

17 D. A. Simpson, E. Morrisroe, J. M. McCoey, A. H. Lombard, D. C. Mendis, F. Treussart, L. T. Hall, S. Petrou and L. C. Hollenberg, *ACS Nano*, 2017, **11**, 12077–12086.

18 R. Tanimoto, T. Hiraiwa, Y. Nakai, Y. Shindo and A. Funahashi, *Sci. Rep.*, 2016, **6**, 22071–22081.

19 J. Zhou, B. Del Rosal, D. Jaque, S. Uchiyama and D. Jin, *Nat. Methods*, 2020, **17**, 967–980.

20 L. Đ. Far and M. D. Dramićanin, *Nanomaterials*, 2023, **13**, 2904–2937.

21 C. Mi, J. Zhou, F. Wang, G. Lin and D. Jin, *Chem. Mater.*, 2019, **31**, 9480–9487.

22 G. P. C. Drummen, *Molecules*, 2012, **17**, 14067–14090.

23 N. Inada, N. Fukuda, T. Hayashi and S. Uchiyama, *Nat. Protoc.*, 2019, **14**, 1293–1321.

24 G. Feng, H. Zhang, X. Zhu, J. Zhang and J. Fang, *Biomater. Sci.*, 2022, **10**, 1855–1882.

25 Y. Sun, M. Fu, M. Bian and Q. Zhu, *Biotechnol. Bioeng.*, 2023, **120**, 7–21.

26 T. Qin, B. Liu, K. Zhu, Z. Luo, Y. Huang, C. Pan and L. Wang, *TrAC, Trends Anal. Chem.*, 2018, **102**, 259–271.

27 B. B. Lowell and B. M. Spiegelman, *Nature*, 2000, **404**, 652–660.

28 X. Han, F. Hu, W. Chi, X. Ma, S. H. Liu, X. Liu and J. Yin, *Sens. Actuators, B*, 2018, **277**, 55–61.

29 T. Liu, J. Huang, H. Ding, C. Zhan and S. Wang, *Spectrochim. Acta, Part A*, 2022, **275**, 121166–121174.

30 H. Wan, Q. Xu, P. Gu, H. Li, D. Chen, N. Li, J. He and J. Lu, *J. Hazard. Mater.*, 2021, **403**, 123656–123674.

31 J. Jenkins, S. M. Borisov, D. B. Papkovsky and R. I. Dmitriev, *Anal. Chem.*, 2016, **88**, 10566–10572.

32 T. Zhao, K. Asawa, T. Masuda, A. Honda, K. Kushiro, H. Cabral and M. Takai, *J. Colloid Interface Sci.*, 2021, **601**, 825–832.

33 A. Vyšniauskas, M. Qurashi, N. Gallop, M. Balaz and H. L. Andersonb, *Chem. Sci.*, 2015, **6**, 5773–5778.

34 T. T. Vu, R. Méallet-Renault, G. Clavier, B. A. Trofimov and M. K. Kuimova, *J. Mater. Chem. C*, 2016, **4**, 2828–2833.

35 A. Vyšniauskas, I. López-Duarte, N. Duchemin, T. Vu, Y. Wu, *et al.*, *Phys. Chem. Chem. Phys.*, 2017, **19**, 25252–25259.

36 A. Vyšniauskas, B. Cornell, P. S. Sherin, K. Maleckaite, M. Kubánková, M. A. Izquierdo, T. T. Vu, Y. A. Volkova, E. M. Budynina, C. Molteni and M. K. Kuimova, *ACS Sens.*, 2021, **6**, 2158–2167.

37 M. M. Ogle, A. D. Smith McWilliams, M. J. Ware, S. A. Curley, S. J. Corr and A. A. Martí, *J. Phys. Chem. B*, 2019, **123**, 7282–7289.

38 J. Luo, Z. Xie, J. W. Y. Lam, L. Cheng, H. Chen, C. Qiu, H. S. Kwok, X. Zhan, Y. Liu, D. Zhu and B. Z. Tang, *Chem. Commun.*, 2001, 1740–1741.

39 R. S. Fernandes and N. Dey, *ACS Appl. Nano Mater.*, 2023, **6**, 5168–5176.

40 T. Li, S. He, J. Qu, H. Wu, S. Wu, Z. Zhao, A. Qin, R. Hu and B. Z. Tang, *J. Mater. Chem. C*, 2016, **4**, 2964–2970.

41 L. Meng, S. Jiang, M. Song, F. Yan, W. Zhang, B. Xu and W. Tian, *ACS Appl. Mater. Interfaces*, 2020, **12**, 26842–26851.

42 Z. Chen, Z. Ding, G. Zhang, L. Tian and X. Zhang, *Molecules*, 2018, **23**, 1725–1737.

43 J. Kwon, M. Elgawish and S. H. Shim, *Adv. Sci.*, 2022, **9**, 2101817–2101841.

44 K. Xue, C. Wang, J. Wang, S. Lv, B. Hao, C. Zhu and B. Z. Tang, *J. Am. Chem. Soc.*, 2021, **143**, 14147–14157.

45 W. Zhang Yuan and Y. Zhang, *J. Polym. Sci., Part A: Polym. Chem.*, 2016, **55**, 560–574.

46 B. Saha, B. Ruidas, S. Mete, C. D. Mukhopadhyay, K. Bauri and P. De, *Chem. Sci.*, 2020, **11**, 141–147.

47 H. Gao, C. Kam, T. Y. Chou, M.-Y. Wu, X. Zhao and S. Chen, *Nanoscale Horiz.*, 2020, **5**, 488–494.

48 H. Xiao, P. Li and B. Tang, *Coord. Chem. Rev.*, 2021, **427**, 213582–213614.

49 M. Hishida, R. Kanno and T. Terashima, *Macromolecules*, 2023, **56**, 7587–7596.

50 K. N. Plunkett, X. Zhu, J. S. Moore and D. E. Leckband, *Langmuir*, 2006, **22**, 4259–4266.

51 C. Gota, K. Okabe, T. Funatsu, Y. Harada and S. Uchiyama, *J. Am. Chem. Soc.*, 2009, **131**, 2766–2767.

52 D. Gong, T. Cao, S.-C. Han, X. Zhu, A. Iqbal, W. Liu, W. Qin and H. Guo, *Sens. Actuators, B*, 2017, **252**, 577–583.

53 J. Qiao, Y.-H. Hwang, D.-P. Kim and L. Qi, *Anal. Chem.*, 2020, **92**, 8579–8583.

54 L. Yin, C. He, C. Huang, W. Zhu, X. Wang, Y. Xu and X. Qian, *Chem. Commun.*, 2012, **48**, 4486–4488.

55 J. Liu, X. Guo, R. Hu, J. Xu, S. Wang, S. Li, Y. Li and G. Yang, *Anal. Chem.*, 2015, **87**, 3694–3698.

56 S. Lin and W. S. Struve, *Photochem. Photobiol.*, 1991, **54**, 361–365.

57 Q. Yu, F. Ding, J. Shen and X. He, *Talanta*, 2021, **228**, 122218–122227.

58 R. Chen, H. Ye, T. Fang, S. Liu, L. Yi and L. Cheng, *Org. Biomol. Chem.*, 2022, **20**, 4128–4134.

59 J. Qiao, C. Chen, L. Qi, M. Liu, P. Dong, Q. Jiang, X. Yang, X. Mu and L. Mao, *J. Mater. Chem. B*, 2014, **2**, 7544–7550.

60 J. Qiao, D. Wu, Y. Song, W. Ji, Q. Yue, L. Mao and L. Qi, *Anal. Chem.*, 2021, **93**, 14743–14747.

61 J. Qiao, Y. H. Hwang, C. F. Chen, L. Qi, P. Dong, X. Y. Mu and D. P. Kim, *Anal. Chem.*, 2015, **87**, 10535–10541.

62 T. Liu and S. Liu, *Anal. Chem.*, 2011, **83**, 2775–2785.

63 K. Okabe, N. Inada, C. Gota, Y. Harada, T. Funatsu and S. Uchiyama, *Nat. Commun.*, 2012, **3**, 705–714.

64 S. Uchiyama, T. Tsuji, K. Ikado, A. Yoshida, K. Kawamoto, T. Hayashi and N. Inada, *Analyst*, 2015, **140**, 4498–4506.

65 S. L. Shen, X. F. Zhang, Y. Q. Ge, Y. Zhu and X. Q. Cao, *Sens. Actuators, B*, 2018, **254**, 736–741.

66 Y. Yuan, R. Zhang, X. Cheng, S. Xu and B. Liu, *Chem. Sci.*, 2016, **7**, 4245–4250.

67 S. Ghosh, Y. F. Chang, D. M. Yang and S. Chattopadhyay, *Biosens. Bioelectron.*, 2020, **155**, 112115–112126.

68 Z. Ding, C. Wang, G. Feng and X. Zhang, *Polymers*, 2018, **10**, 283–293.

69 X. Hu, Y. Li, T. Liu, G. Zhang and S. Liu, *ACS Appl. Mater. Interfaces*, 2015, **7**, 15551–15560.

70 Z. Wang, X. He, T. Yong, Y. Miao, C. Zhang and B. Z. Tang, *J. Am. Chem. Soc.*, 2019, **142**, 512–519.

71 F. Christen, V. Desrosiers, B. A. Dupont-Cyr, G. W. Vandenberg, N. R. Le François, J. C. Tardif, F. Dufresne, S. G. Lamarre and P. U. Blier, *Free Radical Biol. Med.*, 2018, **116**, 11–18.

72 N. Stevic, J. Maalouf, L. Argaud, N. Gallo-Bona, M. Lo Grasso, Y. Gouriou, L. Gomez, C. Crola Da Silva, R. Ferrera, M. Ovize, M. Cour and G. Bidaux, *Cells*, 2022, **11**, 989–1009.

73 R. Zukiene, Z. Nauciene, J. Ciapaite and V. Mildažienė, *Int. J. Hyperthermia*, 2010, **26**, 56–66.

74 E. Carrasco, B. D. Rosal, F. Sanz-Rodríguez, Á. J. D. L. Fuente, D. Jaque, *et al.*, *Adv. Funct. Mater.*, 2015, **25**, 615–626.

75 Z. Huang, N. Li, X. Zhang, C. Wang and Y. Xiao, *Anal. Chem.*, 2018, **90**, 13953–13959.

76 W. Tang, H. Gao, J. Li, X. Wang, Z. Zhou, L. Gai, X. J. Feng, J. Tian, H. Lu and Z. Guo, *Chem.–Asian J.*, 2020, **15**, 2724–2730.

77 D. Chrétien, P. Bénit, C. Leroy, R. El-Khoury, S. Park, J. Y. Lee, Y. T. Chang, G. Lenaers, P. Rustin and M. Rak, *Chemosensors*, 2020, **8**, 124–138.

78 J. SunáYoo, *Chem. Commun.*, 2015, **51**, 8044–8047.

79 X. Liu, T. Yamazaki, H. Y. Kwon, S. Arai and Y. T. Chang, *Mater. Today Bio*, 2022, **16**, 100405–100413.

80 Q. Zhu, Y. Sun, M. Fu, M. Bian, X. Zhu, K. Wang, H. Geng, W. Zeng, W. Shen and Y. Hu, *ACS Sens.*, 2022, **8**, 51–60.

81 M. Homma, Y. Takei, A. Murata, T. Inoue and S. Takeoka, *Chem. Commun.*, 2015, **51**, 6194–6197.

82 F. Shen, W. Yang, J. Cui, Y. Hou and G. Bai, *Anal. Chem.*, 2021, **93**, 13417–13420.

83 T. R. Xie, C. F. Liu and J. S. Kang, *Biophys. Rep.*, 2017, **3**, 85–91.

84 L. Zhang and H. H. Wang, *Dig. Liver Dis.*, 2016, **48**, 709–716.

85 B. Feng, X. Huang, D. Jiang, L. Hua, Y. Zhuo and D. Wu, *Int. J. Mol. Sci.*, 2017, **18**, 1710–1724.

86 A. Ballabio and J. S. Bonifacino, *Nat. Rev. Mol. Cell Biol.*, 2020, **21**, 101–118.

87 R. Kriszt, S. Arai, H. Itoh, M. H. Lee, A. G. Goralczyk, X. M. Ang, A. M. Cypess, A. P. White, F. Shamsi, R. Xue, *et al.*, *Sci. Rep.*, 2017, **7**, 1383–1397.

88 H. Wang, Y. Wu, Y. Shi, P. Tao, X. Fan, X. Su and G. C. Kuang, *Chem.–Eur. J.*, 2015, **21**, 3219–3223.

89 J. Duan, Y. Huang, S. Zong and J. Jiang, *Polymers*, 2020, **13**, 119–133.

90 B. Saha, B. Ruidas, S. Mete, C. D. Mukhopadhyay, K. Bauri and P. De, *Chem. Sci.*, 2020, **11**, 141–147.

91 Z. Zhang, D. Zhang, L. Wei, X. Wang, Y. Xu, H. W. Li, M. Ma, B. Chen and L. Xiao, *Colloids Surf., B*, 2017, **159**, 905–912.

92 D. Wang, H. Huang, M. Zhou, H. Lu, J. Chen, Y. T. Chang, J. Gao, Z. Chai and Y. Hu, *Chem. Commun.*, 2019, **55**, 4051–4054.